

We are IntechOpen, the world's leading publisher of Open Access books Built by scientists, for scientists

4,800

Open access books available

122,000

International authors and editors

135M

Downloads

Our authors are among the

154

Countries delivered to

TOP 1%

most cited scientists

12.2%

Contributors from top 500 universities



WEB OF SCIENCE™

Selection of our books indexed in the Book Citation Index
in Web of Science™ Core Collection (BKCI)

Interested in publishing with us?
Contact book.department@intechopen.com

Numbers displayed above are based on latest data collected.
For more information visit www.intechopen.com



Resistive Switching in Metal Oxide/Organic Semiconductor Nonvolatile Memories

Henrique L. Gomes, Dago M. de Leeuw and
Stefan C.J. Meskers

Additional information is available at the end of the chapter

<http://dx.doi.org/10.5772/intechopen.69023>

Abstract

Diodes incorporating a bilayer of a metal oxide and an organic semiconductor can show unipolar, nonvolatile memory behavior after electroforming. Electroforming involves dielectric breakdown induced by prolonged bias voltage stress. When the power dissipated during breakdown is limited, electroforming is reversible and involves formation of defects at the organic-oxide interface that can heal spontaneously. When the power dissipation during breakdown exceeds a certain threshold, electroforming becomes irreversible. The fully electroformed diodes show electrical bistability, featuring (meta) stable states with low and high conduction that can be programmed by voltage pulses. The high conduction results from current flowing via filamentary paths. The bistability is explained by the coexistence of two thermodynamically stable phases at the interface between semiconductor and oxide. One phase contains mainly ionized defects and has a low work function, while the other phase has mainly neutral defects and a high work function. In the diodes, domains of the phase with low work function give rise to current filaments. In the filaments, Joule heating will raise temperature locally. When the temperature exceeds the critical temperature, the filament will switch off. The switching involves a collective recombination of charge carriers trapped at the defects as evidenced by bursts of electroluminescence.

Keywords: nonvolatile electronic memory, electroforming, unipolar resistive switching, phase transition, critical point

1. Introduction

Metal-insulator-metal (MIM) systems often show electrically induced resistive switching. Diodes of this type have therefore been proposed as replacement of standard NAND-flash

nonvolatile electronic memory [1]. In their pristine state, the materials in the MIM diodes are usually high-resistivity insulators. Before the diodes show memory properties, they have to be electroformed by applying a high electric field in a current-voltage sweep with an appropriate current compliance. This induces a so-called soft breakdown. The electroformed device can be switched between a high conductance on-state and a low conductance off-state as shown in **Figure 1**. The resulting bistable current-voltage (I-V) characteristics can be applied as a nonvolatile memory. A surprisingly large variety of materials and material combinations can give rise to resistive switching [2–9], which indicates that the mechanism of the resistive switching may be very general.

The electric fields needed to induce the electroforming are usually close to the critical field for dielectric breakdown. In practice, the electroforming needs to be tightly controlled by, for example, programming a current compliance limit in the external circuit, in order to avoid permanent shorting and breakdown of the MIM diodes. The yield of active memory cells in the electroforming step is crucial for the success of memristors as a device technology. A detailed understanding of processes happening during electroforming is therefore of paramount importance.

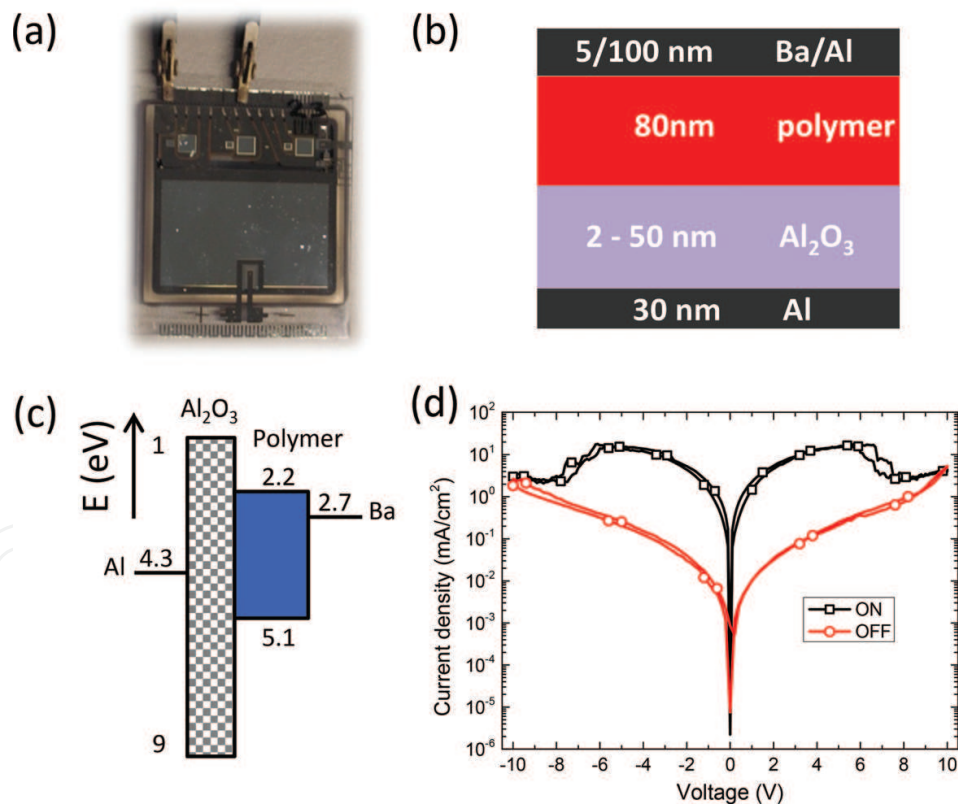


Figure 1. Diode layout. (a) Photograph of device containing several diodes. The devices with an active area of 9 mm^2 were encapsulated to exclude O_2 and H_2O . (b) Typical nominal e-only diode layout where the Al_2O_3 thickness is varied. (c) Flat band diagram where numbers are in eV. (d) J-V characteristics after forming showing a pronounced negative differential resistance.

Resistive switching was first reported in 1962 when Hickmott described a hysteretic I-V characteristic in thin anodic films [10]. A large negative resistance was observed for thin films of SiO_x , Al_2O_3 , Ta_2O_5 , ZrO_2 , and TiO_2 . Early research up to the 1980s has been thoroughly reviewed by Dearnaley et al. [11], by Oxley [12], and by Pagnia and Sotnik [13]. In the 1990s attention shifted from binary oxides to complex metal oxides and has been reviewed by Sawa [14] and by Waser and Aono [15].

The switching mechanism of electroformed diodes can be unipolar or bipolar depending on the type of oxide and the electroforming procedure applied [3]. In unipolar switching, the switching direction depends on the magnitude of applied bias but not on the polarity. The I-V curves of both the on-state and the off-state are symmetric, and the type of electrode is relatively unimportant. In contrast, the switching is called bipolar or antisymmetric when the set of voltage for the on-state occurs at one voltage polarity, while the reset to the off-state occurs at the reversed polarity. The I-V curves are asymmetric and depend on the type of electrode.

Here, we focus on unipolar switching in diodes containing a layer of Al_2O_3 . In order to fabricate reproducible memories, a bilayer comprised of a thin insulating Al_2O_3 layer in series with a semiconducting layer is needed. The yield of active memories made with only an Al_2O_3 layer is extremely low. Electroforming then almost inevitably leads to hard shorts, irrespective of the set of current compliance or of the type of forming, for example, pulsed or voltage sweep. The electrodes melt or even evaporate. Already for the memories made in the 1960s and 1970s, it turned out that an unidentified layer of carbon enhances the reproducibility. Diodes made in high vacuum did not show switching. Oil vapor contamination from a rotary pump was needed to make reliable memories [13].

Reproducible memories with a yield of about unity could be fabricated by adding a well-defined, thin layer of a semiconducting polymer [16]. The devices therefore are often called polymer RRAMs. The type of electrodes turned out to be irrelevant. After electroforming, the I-V characteristics are symmetric. A narrow voltage region with a negative differential resistance (NDR) is observed in both polarities. The device can be switched between a high conductance on-state and a low conductance off-state at biases corresponding to the top and bottom of the NDR. The switching is unipolar and due to the Al_2O_3 . The distributed series resistance of the polymer prevents thermal runaway when a local filament is turned on. Polymer/oxide diodes are then expected not only to exhibit a better control of the switching properties but also to have superior endurance as compared to oxide-only based memristors. In this feature we will show that the semiconducting polymer not only acts as a current-limiting series resistance but that the polymer also plays a crucial role by providing a charged layer of trapped electrons at the polymer/oxide interface. This charge layer enhances the tunneling across the oxide and tunes the formation of electrically bistable defects.

This contribution is an explanatory account of electroforming and unipolar switching in MIM diodes with an internal bilayer structure consisting of Al_2O_3 and a semiconducting polymer

and is organized as follows. In Section 2 we describe investigations into the trapping of charges in pristine diodes and the dielectric breakdown and electroforming that occurs at high bias. In Section 3 we discuss the filamentary nature of the conduction in the diodes and the experimental evidence for this heterogeneous conduction from noise measurements. Finally, Section 4 is devoted to the switching process in the electroformed diodes.

2. Charge trapping and electroforming

Pristine diodes consisting of an Al/Al₂O₃/polyspirofluorene/Ba/Al stack have a large density of empty trap sites for electrons which are located at the interface between the semiconducting polymers. The trap sites can be studied by quasi-static capacitance-voltage (QSCV) measurements [17] and optical detrapping investigations. These measurements provide information on the position and number density of the trap sites.

The QSCV method is ideally suited to study traps that fill quickly but empty slowly. During the measurement, the bias voltage is swept over a certain voltage range and by integrating the current; one keeps track of the number of charges that enter the diode. From the voltage and charge, the capacitance is calculated. **Figure 2** shows the cyclic QSCV scans. First, the voltage is swept over the reverse bias range ($V < 0$). In this range a practically constant capacitance of 30 nF/cm² is recorded which we interpret as the geometrical capacitance, C_0 . The minor hysteresis in the reverse bias range is due to a small leakage current. When subsequently

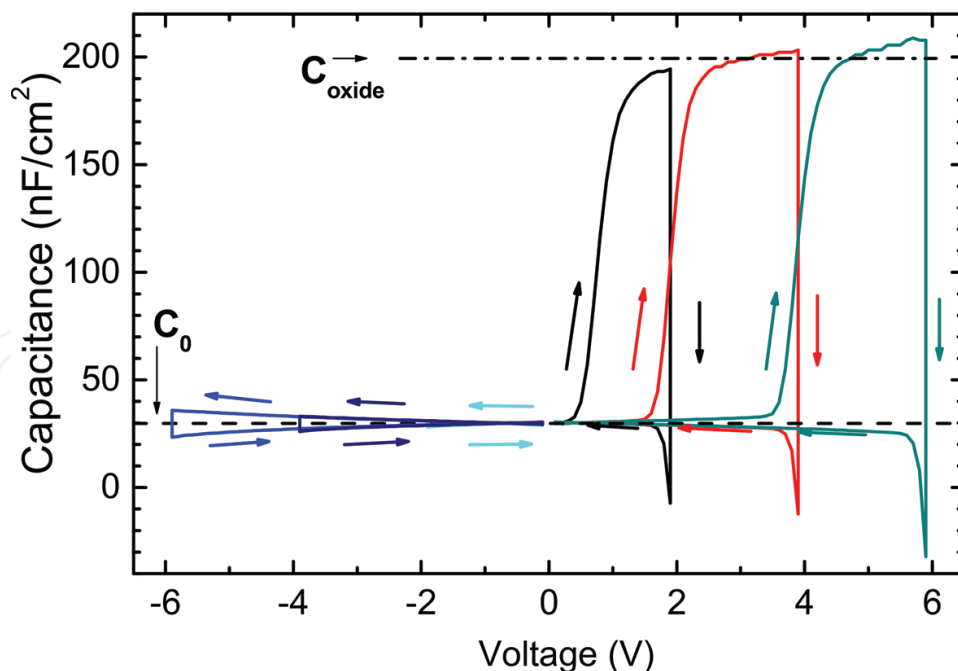


Figure 2. Sequential QSCV characteristics for a Al/Al₂O₃ (40 nm)/polymer(80 nm)/Ba/Al diode measured using an integration time of 4 s and a voltage step of 100 mV. For negative bias voltage V , no charge is injected into the polymer. Both oxide and polymer act as insulators. For positive bias, electrons are injected into the polymer and trapped near the polymer/oxide interface.

sweeping the bias voltage over the forward bias range, a much large hysteresis is observed. When the voltage is swept over a certain range for the first time, a very large capacitance is obtained, which we denote C_{oxide} . Scanning the voltage over the same range but now either in the reverse direction or for a second time in the same direction, the capacitance measured is low and practically equal to C_0 . To account for the anomalously high capacitance values in the first scans, we note that under forward bias electrons can be injected into the semiconducting polymer. These electrons can migrate through the polymer layer under the influence of the applied bias and subsequently get trapped at the polymer/oxide interface. The trap sites are relatively deep, and spontaneous detrapping of the electrons is found to occur on the time scale of days. Detrapping of electrons can be accelerated by illumination with light of photon energy above the bandgap of the semiconducting polymer (3.1 eV).

By varying the thickness of the oxide layer, it can be shown that the anomalous capacitance is inversely proportional to the thickness of the oxide [18, 19]. From the QSCV and optical detrapping experiments [20], it follows that the density of trap sites at the interface exceeds 10^{17} m^{-2} .

Due to the accumulation of electrons at the polymer/oxide interface, the potential difference applied to the diodes as a whole mainly drops over the oxide layer. When increasing the bias voltage over the diode, one will eventually come to a point where the electric field in the oxide exceeds the critical field strength for electrical breakdown, which is estimated at 10^9 V/m for Al_2O_3 [21]. This could lead to catastrophic failure of the diode. In the case of the polymer/oxide diodes, however, the layer of semiconducting polymer acts as current-limiting element, preventing complete or “hard” breakdown of the diodes.

A subtle way of inducing “soft” electrical breakdown in the polymer/oxide diodes is to subject the structure to so-called constant current stress [22]. This is illustrated in **Figure 3**. In the particular example shown, the diode is subjected to a constant current of $1 \mu\text{A}/\text{cm}^2$, and the voltage needed to maintain this current is monitored over time. As can be seen, the voltage that needs to be applied builds up rather quickly over the course of less than a second. This time scale corresponds to complete filling of the trap sites in the diode. When the voltage over the 10-nm-thick oxide reaches 10 V, the critical dielectric strength of the aluminum oxide exceeds, and a sudden, “soft” breakdown occurs. The dielectric breakdown allows the current through the diode to be maintained at much lower applied bias ($V < 1 \text{ V}$).

An intriguing aspect of the “soft” dielectric breakdown shown in **Figure 3** is that the damaged insulator shows spontaneous repair. This “self-healing” is illustrated in **Figure 4**. When monitoring the leakage current through the damaged diode at a relative low applied bias voltage, one finds that the current decreases over time, following a power-law decay. Curiously, the self-healing can be temporarily inhibited, by first emptying the trap sites optically and then keeping the diode at short circuit. After 25 h, the self-healing process can be reactivated by refilling the traps and proceeds with the same kinetics as in the case without inhibition.

The dielectric breakdown under constant current stress has been investigated in more detail. We find that when the electrical power that is dissipated during the breakdown is limited to $0.1 \text{ mW}/\text{cm}^2$, the breakdown is fully reversible. In a tentative explanation, we attribute the breakdown and the subsequent self-healing to quasi-reversible formation of oxygen vacancy

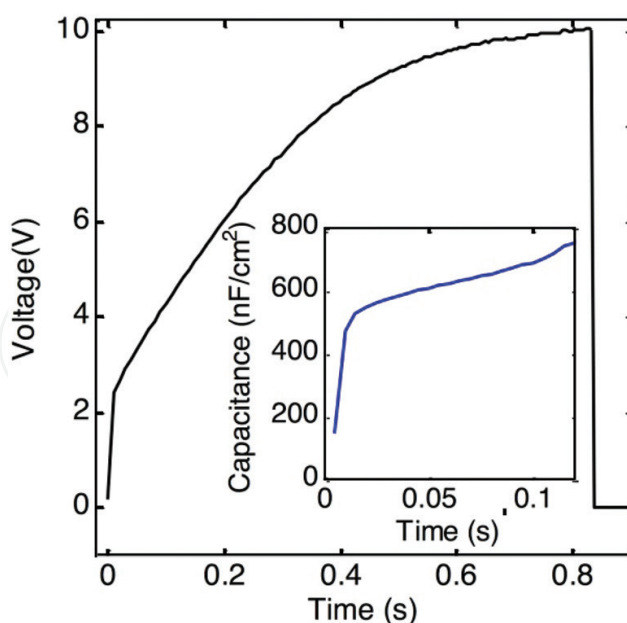


Figure 3. Breakdown under constant current stress. The voltage across the Al/Al₂O₃(20 nm)/polyspirofluorene(80 nm)Ba/Al capacitor as a function of time under a constant current stress of 1 μ A/cm². An abrupt voltage drop is observed at 10 V. The inset shows the corresponding change in capacitance estimated from the change in slope of the voltage.

sites in the oxide near the polymer/oxide interface. This mechanism is described in **Figure 5**. Upon injection of positive charge carriers into the oxide, two oxygen ions dimerize into an O₂ molecule, whereby the electrons are annihilated by the trapped holes. The oxygen vacancies, also referred to as *F*-centers, can exist in a charge neutral state where an electron occupies the

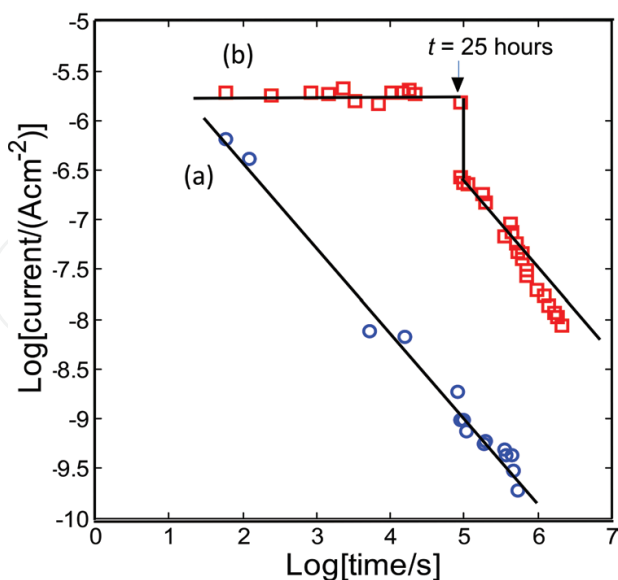


Figure 4. Inhibition of self-healing. Current-time plots for a capacitor electroformed with constant low current stress of 1 μ A. (a) The post-breakdown current probed at 0.5 V bias. The current decays with a power-law dependence on time. (b) The current decay in the same electroformed but now after emptying electron traps with 1000 s illumination with a blue LED ($350 \leq \lambda \leq 650$ nm, $\lambda_{\text{max}} = 440$ nm). After $t = 25$ h triggers, the self-healing process can be reactivated by application of a brief 0–5V voltage ramp to refill the traps.

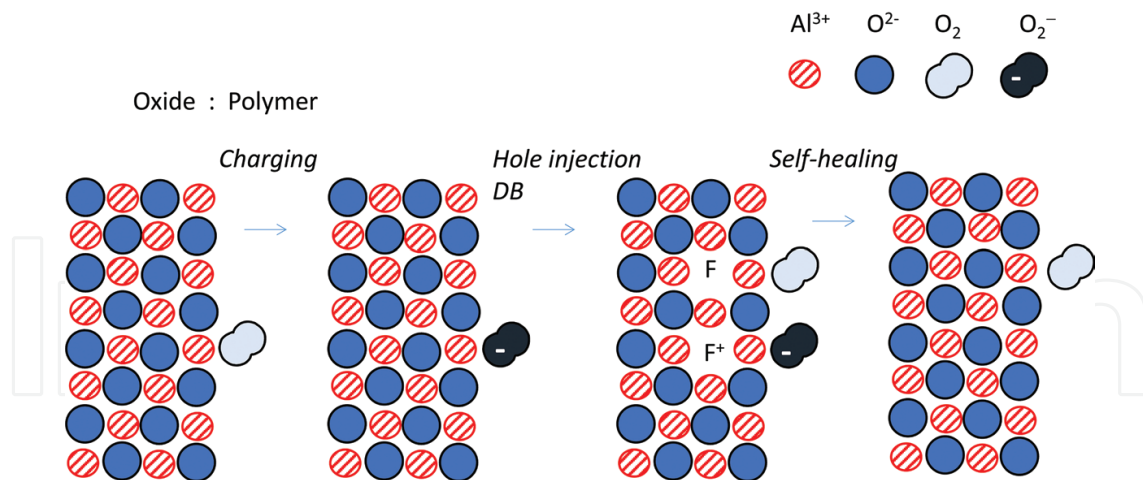


Figure 5. Self-healing mechanism. The hatched and filled spheres represent Al^{3+} and O^{2-} ions of the Al_2O_3 lattice. Neutral oxygen, O_2 , and the superoxide ion, O_2^- are presented by the lemniscates. The first electrons are trapped at the polymer/oxide interface. When the bias is larger than the flat band voltage, holes are injected into the oxide, and a highly polarized electric double layer is formed at the polymer/oxide interface. In dielectric breakdown oxygen vacancies, F-centers are formed. In self-healing, superoxide ions, O_2^- , react with a neutral and charged oxygen vacancy to reform a defect-free Al_2O_3 lattice.

empty space left by the oxygen anion. When the electron leaves the vacancy, the F -center is ionized (F^+). The ionized F^+ center can be regarded as a trapped hole. The O_2 molecules may diffuse into the polymer layer, escape from the electroformed device, or even form oxygen interstitials, depending on the dissipated power used in the electroforming. As long as the O_2 molecules formed in the breakdown process remain close to the interface, we expect the breakdown to be reversible [23]. Due to their large electronegativity, the O_2 molecules trap electrons. The formed superoxide ions, O_2^- , react with a neutral and charged oxygen vacancy to a defect-free Al_2O_3 lattice, indicated by the open square, as



We note that binding of neutral molecular oxygen to n -type metal oxides is a process that occurs in mainly oxides [16, 24, 25], allowing one to monitor oxygen partial pressure through measurement of the electrical resistance. Reversible, electrically induced formation of anion vacancy sites (F -center) in ionic-wide bandgap semiconductors has also been demonstrated for alkali halide-polymer diodes [26–29].

As mentioned above, when the power dissipated during the electrical breakdown is high, the process becomes irreversible, and the diodes are electroformed. We find that the electrical resistance of the electroformed diodes can be switched reversibly by applying voltage pulses.

3. Filamentary conduction and noise measurements

The electrical current in memristor devices is not homogeneous but transported through localized paths or filaments. Evidences have been provided by scanning probe measurement

which confirm the existence of conducting filaments in Al_2O_3 [30, 31] and by an IR-enhanced CCD camera [32]. The spatially resolved thermal images show, in the on-state, hot spots due to highly conductive paths. In the off-state, the spots disappear. However, the spots are not created and destroyed upon switching. Upon repeated switching between the on- and off-states, the same original hot spots were detected in the thermal image. From these observations it has been concluded that upon switching, filaments are neither generated nor destroyed but that individual filaments are turned on and off, like switches.

Relevant information about filament properties is obtained from a detailed electrical characterization. In oxide-/polymer-based memristors, three different behaviors are directly caused by filamentary conduction:

- a. **Electrical noise:** Filaments cause discrete current fluctuations that generate random telegraph like noise and affect the memory reproducibility and scalability.
- b. **Slow response upon repeating switching:** Filaments interact with nearby filaments, and this interaction may slow down the switching speed of a memory device.
- c. **Anomalous temperature dependence of the current:** The mechanism to turn on filaments may lead to a counter-intuitive temperature dependence of the current.

In the next paragraphs, we discuss in detail all the electrical characteristics caused by filamentary conduction.

Electrical noise. Polymer/oxide memristor devices when operating in the on-state show different types of electrical noise depending on the bias point of the I-V curve where it is recorded [33]. For a bias of 0.5 V (ohmic region), the noise follows the $1/f$ dependence (see **Figure 6**). When the diode is biased at higher voltages, in a space-charge-limited (SCL) region, the noise follows a $1/f^{3/2}$ dependence. Hence, a new physical mechanism becomes active at high bias.

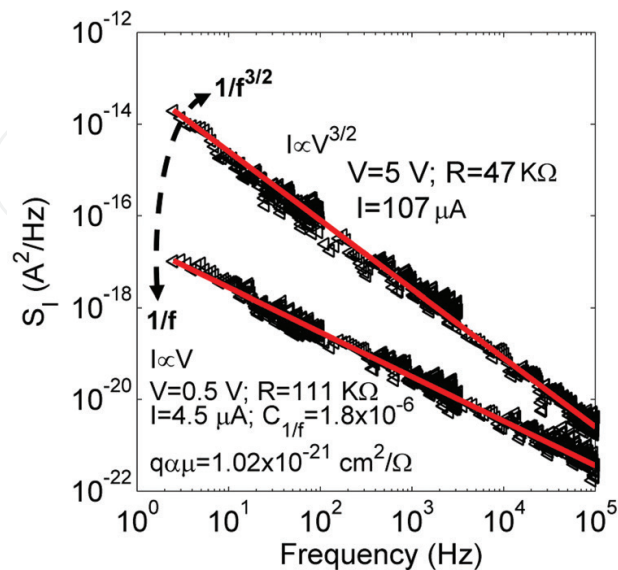


Figure 6. Current noise spectrum in the transition from ohmic to SCL region, indicating a diffusion mechanism at higher bias.

This mechanism is a switching-on and switching-off of conducting channels, at the Al_2O_3 contact. That process dominates the $1/f$ spectrum and the observed slope of the spectrum ($1/f^{3/2}$). Finally, very near to the onset of the NDR region, the noise shows discrete fluctuations like a random telegraph noise (RTN).

Typical time traces from a continuous measurement are presented in **Figure 7**. The time records show large discrete current fluctuations that can reach about 45 nA.

Discrete fluctuations in current-voltage or current-time characteristics appear when charge transport is controlled by the statistical capture/emission of electrons at electron trap sites. Especially when transport occurs through current-carrying filaments, large current fluctuations can occur.

The large discrete current fluctuations allow us to quantify the time that a filament is turned on, τ_{on} , and turned off, τ_{off} . The first and second traces in **Figure 7** exhibit a filamentary path that is most of the time active and only once in a while switches off, with $\tau_{\text{off}} \sim 0.7$ ms. The third trace shows the filament being turned on and turned off at similar time scales of about 1.7 ms. The current fluctuations change their frequency in a random way.

Slow response upon repeating switching. When a memory device is in a high conductive state, there is a large ensemble of filaments. We will show here that when filaments are in relatively close proximity, the switching-on and switching-off of an individual filament not be a totally independent of a filament in the neighborhood. Filaments can interact with each other and contribute to turn on more filaments or even promote a cascade of switching-off events.

It is instructive at this point to investigate the changes in potential distribution and current flow patterns in the diode in the vicinity of a conducting filament. This was achieved using the COMSOL Multiphysics simulator.

In **Figure 8** the device is represented by a simple two-layer structure composed of a thin, high-resistivity oxide layer supporting a thicker, more conductive polymer layer. The color (online) maps represent the potential distributions (blue = -10 V, pink = 0 V) which are further emphasized by superimposed contour lines. In (a) the device is in the off-state; leakage current

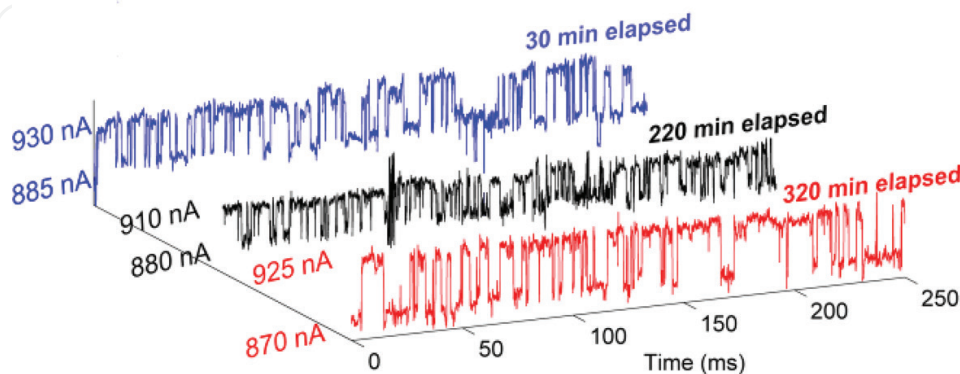


Figure 7. Electrical noise of a memristor programmed in the on-state at $T = 220$ K. The time traces show the current RTN fluctuations under an applied bias near the onset of the NDR region. The time traces were recorded at different times after the start of the measurements (elapsed time).

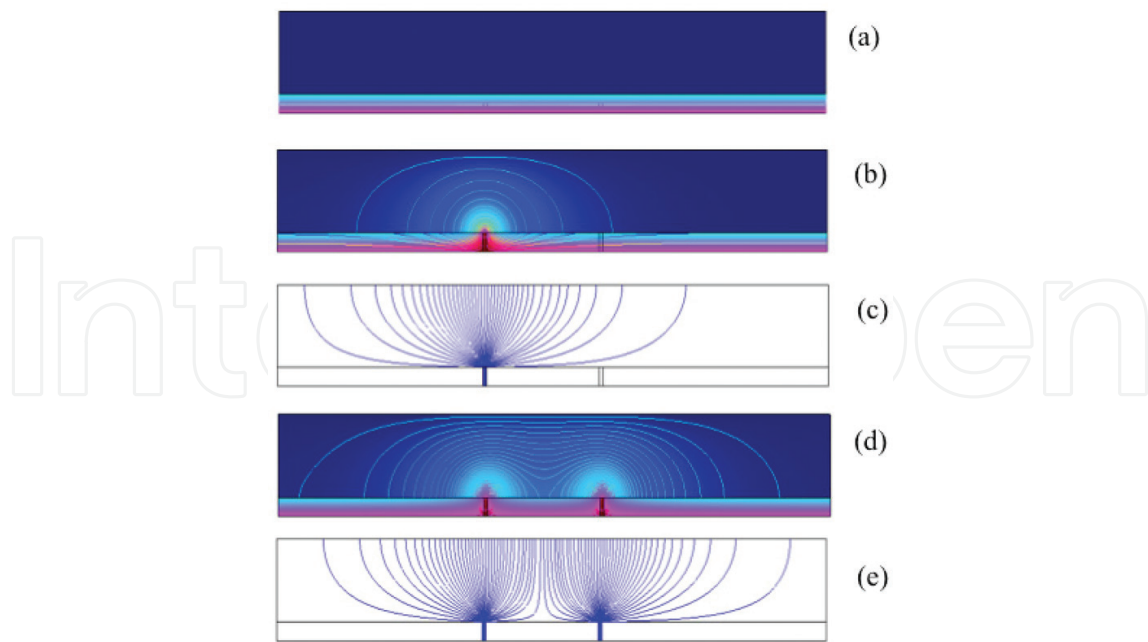


Figure 8. COMSOL simulations showing potential distributions represented both in color (blue = -10 V, pink = 0 V) and by superimposed contour lines (a), (b), (d), and current streamlines (c) and (e) in our two-layer capacitor model. The upper layer represents the polymer and the lower a thin oxide film. (a) Potential distribution in a device in the HRS. The corresponding current streamlines will be vertical and of low density. The changes in potential distribution and current streamlines arising from a single conducting filament in the oxide are shown in (b) and (c). The corresponding distributions for two adjacent filaments are given in (d) and (e).

through the oxide is minimal so that virtually all the applied voltage appears across the oxide layer owing to the higher conductivity of the polymer. Next, we include a conducting filament in the oxide. This results in significant changes in the local potential (b) and in the current density profile (c). We note two important changes:

- (i) The potential at the polymer/oxide interface decreases giving rise to lateral electric fields and extensive distortion of the potential in both the polymer and oxide layers.
- (ii) The current tunnels through the polymer into the filament from a circular area of the electrode whose radius exceeds the polymer film thickness.

In the case of low on-currents, conducting filaments are isolated and well separated. The non-uniform potential distribution (**Figure 8(b)** and **(c)**) allows electrons to be drawn through the polymer from a relatively large area of the electrode. The critical filament current required to effect efficient recombination and turn off the filaments is achieved at relatively low voltages.

For high on-currents, a large number of conducting paths are turned on, many in the neighborhood of an originating filament as discussed above. As seen in **Figure 8(d)** and **(e)**, the electrode area from which electrons are drawn does not increase in proportion to the number of neighboring filaments. Higher voltages will be required then to provide the critical electron current through the polymer for extinguishing these filaments. Consequently, within a volume extending out from the filament into the polymer, considerable Joule heating will occur. Significantly, it is well known that the electrical breakdown strength of most insulating

materials decreases with increasing temperature: a relevant example is soft breakdown in SiO_2 films a few nanometers thick [34]. We postulate that as the applied bias increases, a combination of increasing oxide field and high temperature in the vicinity of the conducting filament triggers the switching of a nearby filament. **Figure 8(d)** and **(e)** shows that the region of disturbed potential and high current density now expands triggering further switching. This process is expected to continue until two local hot spots overlap or expansion becomes limited by the process(es) leading to the NDR. Even if further filamentary conduction is not initiated, additional thermally induced currents will flow in both the polymer and oxide leading to a similar expansion of the hot spot.

Anomalous temperature dependence of the current. The I-V characteristics for the on-state show a large increase in the magnitude of the current upon lowering the temperature of the diodes. This behavior is illustrated in **Figure 9**. The increase of current is more pronounced at higher bias voltages, in the voltage range below the sharp onset of the NDR.

To further explore this unusual temperature dependence, a diode was programmed into the on-state at room temperature and then cooled down until 120 K. Meanwhile, the current transient was recorded while applying a continuous bias voltage (2 V). The magnitude of the current increases more than double in a temperature range of 200°C, as illustrated in **Figure 10**. This observation corresponds to a positive temperature coefficient (PTC) [35–37] of the electrical resistivity, $\alpha \approx 0.01 \text{ K}^{-1}$, an anomalously large value when compared with typical values for metals ($\alpha = 0.0039 \text{ K}^{-1}$ for Cu). On the basis of the anomalously large PTC, it contradicts the explanations based on a metallic type of conduction.

The large and stepwise increase in current indicates that by lowering the temperature some filaments can be activated. In the next section, we provide a tentative explanation for this remarkable experimental observation.

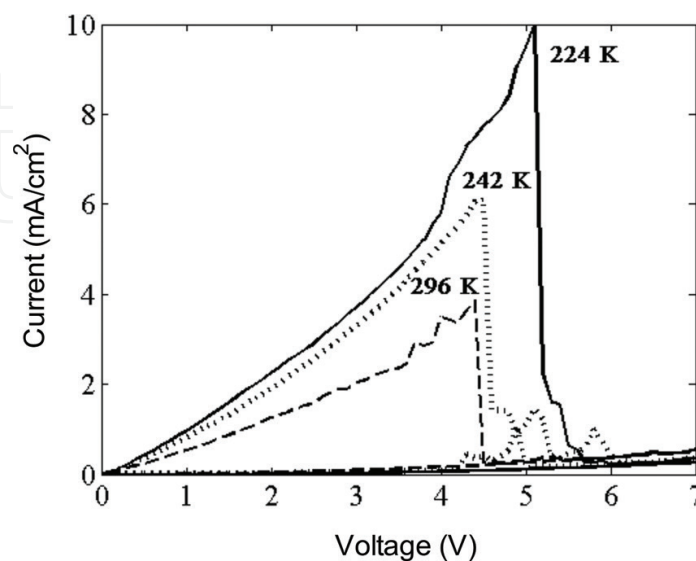


Figure 9. Temperature dependence of the I-V curve of a diode programmed into the on-state.

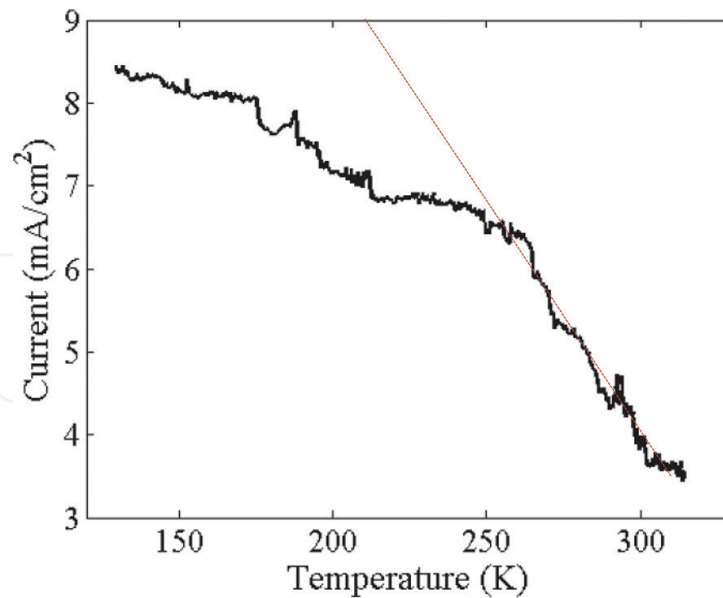


Figure 10. Temperature dependence of the I-V curve of a diode programmed into the on-state monitored at 2 V. The cooling speed is 1 K/min.

4. Electroluminescence and filament model

A key experimental observation in unraveling the mechanism of the nonvolatile electronic memory effects in aluminum oxide has been the occurrence of *electroluminescence* in the visible range of the spectrum during the switching [10, 38]. This observation provides direct experimental evidence that recombination of positive and negative charge carriers takes place at defects in the oxide. Furthermore, it has also been reported that electroformed oxide layers can emit electrons into the vacuum [11]. The latter observations show that an electroformed oxide layer on a metal can dramatically alter the work function of the underlying metal [39, 40].

In **Figure 11** we illustrate the occurrence of electroluminescence in electroformed Al_2O_3 /polyfluorene diodes during switching. Starting at zero bias in the high conduction state, the current density rises rapidly with increasing bias. For voltages above 4 V, the diode shows negative differential resistance (NDR), and the current density actually decreases with increasing bias voltage. In the voltage range corresponding to the NDR behavior, the diode also shows irregular electroluminescence. Light is emitted during a series of short bursts. At high bias voltage ($V > 10$ V), the diodes show more steady light emission.

In order to account for the filamentary conduction and the electroluminescence, we propose that in the diode clusters of charged defects at the polymer/oxide interface are present. We propose a charged bilayer arrangement of charges with, for example, positively charged defects in the oxide compensated by trapped electrons on the polymer side of the interface. The double-layer arrangement locally changes the work function of the electrodes and

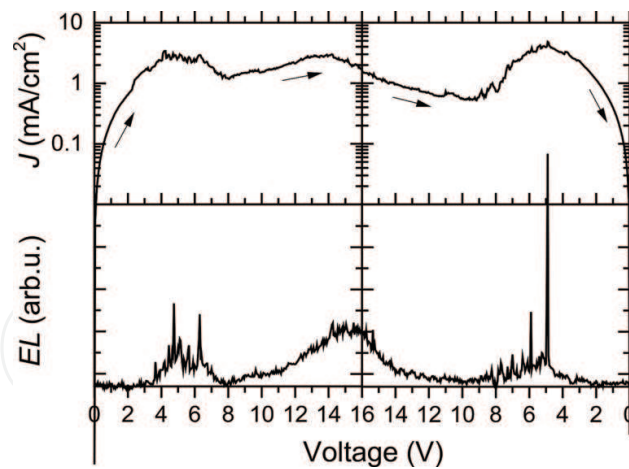


Figure 11. Electroluminescence. (Upper panel) current density (J) and (lower panel) electroluminescence (EL) intensity recorded simultaneously for an electroformed ITO/ Al_2O_3 (10 nm)/polyfluorene (80 nm)/Ba/Al diode during a voltage sweep from 0 V \rightarrow 16 V \rightarrow 0 V.

allows current to flow at already low bias voltages. The local spots on the oxide layer where the effective work function has been altered give rise to current filamentary currents in the diode (see **Figure 12**). We note that formation of charged double layers near metal electrodes is well known in wet electrochemistry [41, 42].

To explain the electrical bistability of the nonvolatile memories, we propose the coexistence of two thermodynamically stable phases in the electroformed oxide layer [26]. The two phases occur in the quasi-two-dimensional double layer consisting of trapped electrons in the organic semiconductor and holes trapped at defects in the metal oxide. One phase containing mainly ionized defects has a low work function. The other phase comprises mainly defects in their neutral state and has a high work function. In the diodes, domains of the phase with low work function constitute current filaments.

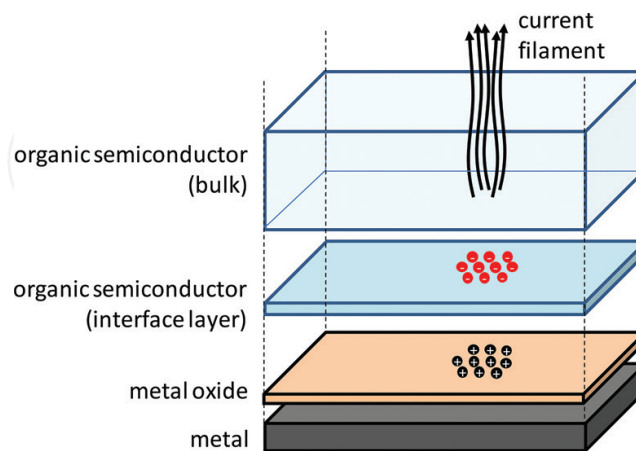


Figure 12. Schematic representation of current filament. In the electroformed diode, ionizable defects are present near the oxide/organic semiconductor interface with a number density above a critical limit. Due to cooperative interaction between the defects, the diode is electrically bistable. Arrays of mainly neutral defects have a high work function and constitute the off-state. Arrays of mainly ionized defects have a low work function and constitute the on-state.

In order to better explain the proposed thermodynamic bistability, we draw on an analogy with saturated salt solutions. Charged ions in such a system can be present in two phases, one where the ions are dispersed throughout the solutions and another phase where ions of opposite charge have condensed into a crystal. As is well, cooperative interactions between the oppositely charged ions give rise to crystallization of salt, for example, NaCl.

In rock salt, the positive and negative ions are packed in a cubic lattice (see **Figure 13**). If we however cut the crystal under an oblique angle, for example, parallel to the (1 1 1) plane, one sees that the crystal actually consists of layers of oppositely charged ions.

For the electroformed oxide layers, we argue that, provided neutral defect sites which are available with sufficient density, electrical charges that have been injected into the diode may condense spontaneously at the polymer/oxide interface due to their mutual electrostatic stabilization. By detailed consideration of the Coulomb interaction potentials of the charge defects, it can be shown that also the image charges in the nearby metal electrode contribute to the stabilization. The condensation of the charges can be mapped onto the 2D Ising model. Based on the 2D Ising model, one predicts that in analogy to ferromagnetism, a critical temperature T_c should exist. For temperatures lower than T_c , the coexistence of two thermodynamically stable phases is predicted. One of the phases should have mainly ionized defects and the other predominantly neutral defects. The magnitude of T_c depends on the strength of the interactions between the sites and should therefore be influenced by the density of defect states.

In order to explain the switching-off of current filaments, we argue that Joule heating associated with the current through the filaments in the oxide will cause the temperature in the oxide layer to rise locally. Once the temperature is above T_c , the mutual stabilization of charges is compromised, and sudden massive recombination of charges occurs. This recombination may account for the bursts of electroluminescence that can be observed during the switching process (see **Figure 11**). Furthermore, recombination of charges in the oxide layer will result in changes in the effective internal work function of the electrodes. This may account for the experimental observation of changes in the built-in potential of an electroluminescent diode during electrically induced breakdown [43].

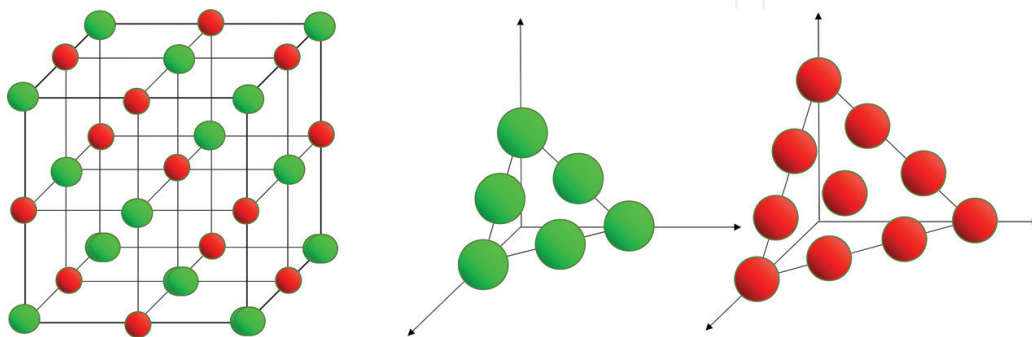


Figure 13. Crystal structure of rock salt (NaCl). Ions of the same charge are packed in layers that lie parallel to the (1 1 1) plane.

5. Conclusion

Unipolar switching in Al_2O_3 diodes involves defects that are created during the electroforming step. The density of defects is critical to the memory operation. Reproducible electroforming is possible by including in the device a well-defined thin layer of a semiconducting polymer. In their pristine state, the polymer/oxide diodes are insulating. The purpose of the polymer layer is threefold. Firstly, the polymer layer acts as a current-limiting series resistance that prevents thermal runaway during electroforming. Secondly, the presence of the polymer introduces an internal polymer/oxide interface, where electrons can accumulate. The trapped electrons stabilize positively charged defects that are generated during electroforming by electrostatic interactions. The trapped electrons promote injection of holes into the oxide, yielding a soft breakdown. Molecular oxygen is expelled and oxygen vacancies are formed. The third purpose of the polymer in the diode is to buffer the molecular oxygen formed.

The experimental evidence indicates that the density of defects in the metal-insulator-metal diodes is of crucial importance to obtain a memory diode with nonvolatile memory properties. If the defect density is too high, the diode will be low. If the density is too low, the critical temperature T_c for phase coexistence is also low. At temperatures $T > T_c$, phase coexistence is not possible, and the memory diode does not show electrical bistability. Upon cooling down, additional filaments should switch on as soon as the temperature drops below the T_c associated with the locale defect density near the filament. This prediction is supported by the experiments in Section 2. Noise measurements prove a unique tool to characterize the dynamics of the defect ionization and neutralization. The onset of discrete fluctuations and random telegraph signals may serve as a diagnostic to determine the difference between the actual defect density and the desired concentration for memory operation.

In summary, unipolar resistive switching poses a unique challenge to the materials that scientists design, deposit, and characterize with appropriate electronic structure, defect ordering, and internal charge carrier dynamics. This challenge seems parallel to development of, e.g., materials for high-temperature superconductivity. Fortunately, in the case of memristors, we have already the certainty from the present state of the art involving the electroforming that relatively simple materials exist with the required properties. The challenge is to gain control over the now largely random process of defect formation.

Author details

Henrique L. Gomes^{1,2*}, Dago M. de Leeuw³ and Stefan C.J. Meskers⁴

*Address all correspondence to: hgomes@ualg.pt

1 Instituto de Telecomunicações, Lisboa, Portugal

2 Universidade do Algarve, Faro, Portugal

3 Smart Materials, Delft University of Technology, The Netherlands

4 Molecular Materials and Nanosystems and Institute for Complex Molecular Systems, Eindhoven University of Technology, Eindhoven, The Netherlands

References

- [1] Chen A, Hutchby J, Zhirnov VV, Bourianoff G, editors. *Emerging Nanoelectronic Devices*. 1st ed. New York: Wiley; 2015. 540 p. DOI: 10.1002/9781118958254
- [2] Yang Y, Ouyang J, Ma L, Tseng RJ-H, Chu C-W. Electrical switching and bistability in organic/polymeric thin films and memory devices. *Advanced Functional Materials*. 2006;**16**(8):1001-1014. DOI: 10.1002/adfm.200500429
- [3] Scott JC, Bozano LD. Nonvolatile memory elements based on organic materials. *Advanced Materials*. 2007;**19**(11):1452-1463. DOI: 10.1002/adma.200602564
- [4] Cho B, Kim T-W, Song S, Ji Y, Jo M, Hwang H, Jung G-Y, Lee T. Rewritable switching of one diode–one resistor nonvolatile organic memory devices. *Advanced Materials*. 2010;**22**(11):1228-1232. DOI: 10.1002/adma.200903203
- [5] Cho B, Song S, Ji Y, Kim T-W, Lee T. Organic resistive memory devices: Performance enhancement, integration, and advanced architectures. *Advanced Functional Materials*. 2011;**21**(15):2806-2829. DOI: 10.1002/adfm.201100686
- [6] Lin WP, Liu SJ, Gong T, Zhao Q, Huang W. Polymer-based resistive memory materials and devices. *Advanced Functional Materials*. 2014;**26**(4):570-606. DOI: 10.1002/adma.201302637
- [7] Heremans P, Gelinck GH, Müller R, Baeg K-J, Kim D-Y, Noh Y-Y. Polymer and organic nonvolatile memory devices. *Chemistry of Materials*. 2010;**23**(3):341-358. DOI: 10.1021/cm102006v
- [8] Liaw D-J, Wang K-L, Huang Y-C, Lee K-R, Lai J-Y, Ha C-S. Advanced polyimide materials: Syntheses, physical properties and applications. *Progress in Polymer Science*. 2012;**37**(7):907-974. DOI: 10.1016/j.progpolymsci.2012.02.005
- [9] Kurosawa T, Higashihara T, Ueda M. Polyimide memory: A pithy guideline for future applications. *Polymer Chemistry*. 2013;**4**(1):16-30. DOI: 10.1039/C2PY20632C
- [10] Hickmott TW. Low-frequency negative resistance in thin anodic oxide films. *Journal of Applied Physics*. 1962;**33**(9):2669-2682. DOI: 10.1063/1.1702530
- [11] Dearnaley G, Stoneham AM, Morgan DV. Electrical phenomena in amorphous oxide films. *Reports on Progress in Physics*. 1970;**33**(3):1129-1191. DOI: 10.1088/0034-4885/33/3/306
- [12] Oxley DP. Electroforming, switching and memory effects in oxide thin films. *Electrocomponent Science and Technology*. 1977;**3**(4):217-224. DOI: 10.1155/APEC.3.217
- [13] Pagnia H, Sotnik N. Bistable switching in electroformed metal–insulator–metal devices. *Physica Status Solidi (a)*. 1988;**108**(1):11-65. DOI: 10.1002/pssa.2211080102
- [14] Sawa A. Resistive switching in transition metal oxides. *Materials Today*. 2008;**11**(6):28-36. DOI: 10.1016/S1369-7021(08)70119-6

- [15] Waser R, Aono M. Nanoionics-based resistive switching memories. *Nature Materials*. 2007;**6**(11):833-840. DOI: 10.1038/nmat2023
- [16] Verbakel F, Meskers SCJ, Janssen RAJ, Gomes HL, Cölle M, Büchel M, De Leeuw DM. Reproducible resistive switching in nonvolatile organic memories. *Applied Physics Letters*. 2007;**91**(19):192103. DOI: 10.1063/1.2806275
- [17] Ziegler K, Klausmann E. Static technique for precise measurements of surface potential and interface state density in MOS structures. *Applied Physics Letters*. 1975;**26**(7):400-402. DOI: 10.1063/1.88193
- [18] Bory BF, Meskers SCJ, Janssen RAJ, Gomes HL, De Leeuw DM. Trapping of electrons in metal oxide-polymer memory diodes in the initial stage of electroforming. *Applied Physics Letters*. 2010;**97**(22):222106. DOI: 10.1063/1.3520517
- [19] Gomes HL, Da Costa AMR, Moreira JA, De Leeuw DM, Meskers SCJ. The role of internal structure in the anomalous switching dynamics of metal-oxide/polymer resistive random access memories. *Thin Solid Films*. 2012;**522**:407-411. DOI: 10.1016/j.tsf.2012.08.041
- [20] Chen Q, Bory BF, Kiazadeh A, Rocha PRF, De Leeuw DM, Meskers SCJ. Opto-electronic characterization of electron traps upon forming polymer oxide memory diodes. *Applied Physics Letters*. 2011;**99**(8):083305. DOI: 10.1063/1.3628301
- [21] Verbakel F, Meskers SCJ, Janssen RAJ, Gomes HL, van den Biggelaar AJM, de Leeuw DM. Switching dynamics in non-volatile polymer memories. *Organic Electronics: Physics, Materials, Applications*. 2008;**9**(5):829-833. DOI: 10.1016/j.orgel.2008.05.022
- [22] Chen Q, Gomes HL, Rocha PRF, De Leeuw DM, Meskers SCJ. Reversible post-breakdown conduction in aluminum oxide-polymer capacitors. *Applied Physics Letters*. 2013;**102**(15):153509. DOI: 10.1063/1.4802485
- [23] Verbakel F, Meskers SCJ, Janssen RAJ. Electronic memory effects in diodes from a zinc oxide nanoparticle-polystyrene hybrid material. *Applied Physics Letters*. 2006;**89**(10):102103. DOI: 10.1063/1.2345612
- [24] Verbakel F, Meskers SCJ, Janssen RAJ. Electronic memory effects in diodes of zinc oxide nanoparticles in a matrix of polystyrene or poly(3-hexylthiophene). *Journal of Applied Physics*. 2007;**102**(8):083701
- [25] Verbakel F, Meskers SCJ, Janssen RAJ. Surface modification of zinc oxide nanoparticles influences the electronic memory effects in ZnO-polystyrene diodes. *Journal of Physical Chemistry C*. 2007;**111**(28):10150-10153. DOI: 10.1021/jp072999j
- [26] Bory BF, Rocha PRF, Gomes HL, De Leeuw DM, Meskers SCJ. Unipolar resistive switching in metal oxide/organic semiconductor non-volatile memories as a critical phenomenon. *Journal of Applied Physics*. 2015;**118**(20):205503. DOI: 10.1063/1.4936349
- [27] Rocha PRF, Gomes HL, Asadi K, Katsouras I, Bory B, Verbakel F, Van De Weijer P, De Leeuw DM, Meskers SCJ. Sudden death of organic light-emitting diodes. *Organic Electronics: Physics, Materials, Applications*. 2015;**20**:89-96. DOI: 10.1016/j.orgel. BF, Wang J, Gomes HL, Janssen RAJ, De Leeuw 2015.02.009

- [28] Bory DM, Meskers SCJ. Relation between the electroforming voltage in alkali halide-polymer diodes and the bandgap of the alkali halide. *Applied Physics Letters*. 2014;**105**(23):233502. DOI: 10.1063/1.4903831
- [29] Bory BF, Rocha PRF, Janssen RAJ, Gomes HL, De Leeuw DM, Meskers SCJ. Lithium fluoride injection layers can form quasi-Ohmic contacts for both holes and electrons. *Applied Physics Letters*. 2014;**105**(12):123302. DOI: 10.1063/1.4896636
- [30] Kurnosikov O, De Nooij FC, LeClair P, Kohlhepp JT, Koopmans B, Swagten HJM, De Jonge WJM. STM-induced reversible switching of local conductivity in thin. *Physical Review B*. 2001;**64**(15):1534071-1534074. DOI: 10.1103/PhysRevB.64.153407
- [31] Kim YS, Kim J-S, Choi JS, Hwang IR, Hong SH, Kang S-O, Park BH. Resistive switching behaviors of NiO films with controlled number of conducting filaments. *Applied Physics Letters*. 2011;**98**(19):192104. DOI: 10.1063/1.3589825
- [32] Cölle M, Büchel M, de Leeuw DM. Switching and filamentary conduction in non-volatile organic memories. *Organic Electronics: Physics, Materials, Applications*. 2006;**7**(5):305-312. DOI: 10.1016/j.orgel.2006.03.014
- [33] Rocha PRF, Gomes HL, Vandamme LKJ, Chen Q, Kiazadeh A, De Leeuw DM, Meskers SCJ. Low-frequency diffusion noise in resistive-switching memories based on metal-oxide polymer structure. *IEEE Transactions on Electron Devices*. 2012;**59**(9):2483-2487/6243198. DOI: 10.1109/TED.2012.2204059
- [34] Lombardo S, Stathis JH, Linder BP, Pey KL, Palumbo F, Tung CH. Dielectric breakdown mechanisms in gate oxides. *Journal of Applied Physics*. 2005;**98**(12):121301. DOI: 10.1063/1.2147714
- [35] Chen L, Xia Y, Liang X, Yin K, Yin J, Liu Z, Chen Y. Nonvolatile memory devices with Cu₂S and Cu-Pc bilayered films. *Applied Physics Letters*. 2007;**91**(7):073511. DOI: 10.1063/1.2771064
- [36] Joo W-J, Choi T-L, Lee K-H, Chung Y. Study on threshold behavior of operation voltage in metal filament-based polymer memory. *Journal of Physical Chemistry B*. 2007;**111**(27):7756-7760. DOI: 10.1021/jp0684933
- [37] Gomes HL, Rocha PRF, Kiazadeh A, De Leeuw DM, Meskers SCJ. Anomalous temperature dependence of the current in a metal-oxide-polymer resistive switching diode. *Journal of Physics D: Applied Physics*. 2011;**44**(2):025103. DOI: 10.1088/0022-3727/44/2/025103
- [38] Hickmott TW. Millimeter distance effects of surface plasmon polaritons in electroformed Al-Al₂O₃-Ag diodes. *Journal of Applied Physics*. 2017;**121**:083101. DOI: 10.1063/1.4976715
- [39] Biederman H. Metal-insulator-metal sandwich structures with anomalous properties. *Vacuum*. 1976;**26**(11):513-523. DOI: 10.1016/S0042-207X(76)81130-X
- [40] Eckertová L. Feldkathoden mit dünnen Isolatorschichten. *Physica Status Solidi (B)*. 1966;**18**(1):3-40. DOI: 10.1002/pssb.19660180102

- [41] Fedorov MV, Kornyshev AA. Ionic liquids at electrified interfaces. *Chemical Reviews*. 2014;**114**(5):2978-3036. DOI: 10.1021/cr400374x
- [42] Healy TW, Scales PJ. The oxide water interface: How valid is the site dissociation surface equilibria model. *Chemistry Letters*. 2012;**41**(10):1020-1022. DOI: 10.1246/cl.2012.1020
- [43] Bory BF, Gomes HL, Janssen RAJ, De Leeuw DM, Meskers SCJ. Electrical conduction of LiF interlayers in organic diodes. *Journal of Applied Physics*. 2015;**117**(15):155502. DOI: 10.1063/1.4917461

IntechOpen

